Effect of Cl⁻ ions and benzylideneacetone/ethanol on the underpotential deposition of zinc in acidic media: cyclic voltammetry and EQCM studies

P.F. Méndez[a], J.R. López[a], Y. Meas[a], R. Ortega[a], L. Salgado[b], G. Trejo[a],*

[a] Centro de Investigación y Desarrollo Tecnológico en Electroquímica (CIDETEQ), Parque Tecnológico Sanfandila,
Pedro Escobedo, A. P. 064. Querétaro C.P. 76700, Mexico
[b] Universidad Autónoma Metropolitana, Area de Electroquímica. Apdo. Postal 55-534, México D.F. 09340, Mexico

Abstract

The influence of chloride ions and a benzylideneacetone (BDA)/ethanol (EtOH) mixture on the underpotential deposition (UPD) of Zn^{2+} ions on Pt electrodes in acidic media was investigated by cyclic voltammetry and electrochemical quartz crystal microbalance (EQCM). In the potential region of the UPD of H and Zn, the surface coverage of Zn adatoms on Pt was evaluated based on the correspondence between charge and mass for several different solutions. In the absence of Cl⁻ ions and BDA/EtOH, the maximum surface coverage of the Zn deposited by UPD was 0.29. In addition, in the presence of Cl⁻ ions, the UPD of Zn^{2+} ions occurred simultaneously with the adsorption of Cl⁻, and the presence of Cl⁻ did not modify the quantity of Zn deposited by UPD. In the presence of Cl⁻ ions and BDA/EtOH, the maximum surface coverage of the Zn deposited by UPD was 0.16. The partial inhibition of the UPD of Zn^{2+} ions is associated with the adsorption of BDA/EtOH or products of the decomposition of BDA/EtOH during the UPD process.
© 2004 Elsevier Ltd. All rights reserved.

Keywords: Additives; Benzylideneacetone; EQCM; Zinc underpotential deposition

1. Introduction

Coatings of zinc and its alloys are of great practical importance due to their capacity to protect ferrous substrates against corrosion [1–4]. Various factors affect the mechanism of zinc electrodeposition, and hence influence the composition and morphology of the coatings obtained. These factors include the concentration of zinc ions [5], complexing agents [6], anions [7,8], and additives [9], all of which play fundamental roles in zinc electrodeposition. The use of additives in electrolytic baths is very important due to their influence on the growth and structure of the deposits obtained. Typically, additives are added to the electrolytic bath at concentrations on the order of parts per million and their presence promotes the formation of soft and shiny coatings. In recent years, mixtures of benzylideneacetone (BDA) and ethanol (EtOH) have been increasingly used as an additive in the electrodeposition of zinc [10–13] and Zn–Co alloy coatings in acidic electrolytic baths [14]. The superior quality of the coatings obtained in the presence of BDA/EtOH has generated growing interest in the mechanism by which this additive affects zinc electrodeposition. However, despite the work carried out in this area, the adsorption characteristics of BDA/EtOH and its mechanism of action during electrodeposition remain largely unknown. One potentially useful method for obtaining information on the function of BDA/EtOH during electrodeposition is to study the formation of the initial states of the deposit, that is, the underpotential deposition (UPD) of Zn^{2+} ions under the influence of the organic additive.

The UPD of Zn^{2+} ions has been studied by Aramata and coworkers [15,16] on polycrystalline and monocrystalline Pt, Pd and Au substrates. They investigated the effect of pH on the anodic displacement of the peak corresponding to the dissolution of Zn deposited by UPD onto Pt, and suggested that the UPD of Zn^{2+} ions on Pt involves the transfer of two electrons. In addition, it has been reported that the UPD of Zn^{2+} ions is sensitive to the crystallographic orientation of the surface, with the (1 1 0) orientation being the most favored [17].

The influence of anions on UPD of Zn^{2+} ions has been studied by various groups. Taguchi and Aramata [18] studied the UPD of Zn^{2+} in phosphate media by cyclic voltammetry. They proposed a model involving three stages: (i) desorption of anions from the substrate, (ii) UPD of Zn^{2+} ions, and (iii) adsorption of anions onto the Zn deposited by UPD. This model is supported by results obtained using voltammetry [18], the radiotracer technique [19,20], FT-IR, and EQCM [21]. In addition, Taguchi and Aramata [18] demonstrated that the adsorption of Cl^-, HSO_4^- (SO_4^{2-}) and $H_2PO_4^-$ onto Pt is induced by the coadsorption of adatoms of Zn. The results show that the specific adsorption of HSO_4^- (SO_4^{2-}) and $H_2PO_4^-$ ions onto the Zn adatoms is greater than the adsorption of Cl^- ions. In a study using voltammetry and rotating ring-disc voltammetry, Mascaro et al. [22] showed that the coadsorption of HSO_4^-, ClO_4^- and F^- onto the substrate (Pt) or adatoms influenced the nature of the Zn adlayer.

Previous studies of the UPD of Zn^{2+} ions have shed light on the fundamental aspects of this process, including effects related to the nature of the substrate, crystallographic orientation of the surface, pH of the solution, and the anions. However, only limited information is available regarding the influence of organic compounds in the electrolytic medium on UPD of Zn^{2+} ions. The study of UPD Zn^{2+} ions in electrolytic media similar to the baths used for massive deposition should contribute valuable information that will aid in elucidating the action of these species in the Zn deposition process. The aim of the present work was to study the UPD of Zn^{2+} ions onto Pt electrodes in acid media under the influence of chloride ions and BDA/EtOH. This study was carried out using cyclic voltammetry in conjunction with EQCM.

2. Experimental

The electrogravimetric study was performed in a conventional three electrode cell with a water jacket. An EQCM (Maxtek, Mod. 710) and a potentiostat/galvanostat (PAR, Mod. 273A) controlled by independent computers running the software PM710 and M270, respectively, were used to simultaneously record electrochemical measurements and the resonance frequency of the quartz crystal. An AT-cut quartz crystal of nominal frequency $f_0 = 5$ MHz, covered on both

sides with a platinum film (Maxtek) was used as the working electrode (Pt-EQCM). The geometric area of the platinum electrode (Pt-EQCM) was $1.37\,cm^2$. The real area of the Pt-EQCM electrode was estimated from the desorption charge of H UPD and the charge corresponding to the value predicted for the desorption of a monolayer of H_{ads} from polycrystalline platinum ($0.210\,mC\,cm^{-2}$) [23]. The value obtained for the real area was $8.05\,cm^2$ and the roughness factor, f_r, was found to be 5.9.

The EQCM signal was recorded as $\Delta f\,(=f-f_0)$ as a function of the electrode potential. The relation between the change in surface mass and the resonance frequency for an EQCM electrode is given by the Sauerbrey equation [24]:

$$\Delta f = -C_f \Delta m \tag{1}$$

where Δf (Hz) is the frequency change, Δm ($ng\,cm^{-2}$) the mass change per unit area, and C_f ($Hz\,ng^{-1}\,cm^2$) is the sensitivity factor of the quartz crystal used for the measurements. The value of C_f was determined in independent experiments on the Faradaic deposition of Ag onto the Pt-EQCM electrode ($C_f = 0.051\,Hz\,ng^{-1}\,cm^2$). Recently, Vatankhah et al. [25] reported that the value of C_f for Pt-EQCN electrodes depended on the electrochemical technique used, as well as on the thickness of the deposited Ag film. They suggested that an adequate experimental procedure for determining C_f could be based on chronopotentiometric or chronoamperometric measurements and Ag deposits on the order of 7–16 monolayer equivalents. In the present work, chronoamperometry was used to obtain the value of C_f. The Ag deposits were obtained using a solution comprised of 10^{-2} M $AgNO_3$ in 0.2 M H_2SO_4. The potential was stepped from an initial value, $E_i = 0.7$ V, to the final one, $E_f = 0.51$ V versus NHE. The time of duration of the step went between 10 and 150 s. In the series of experiments, the changes in the frequency response were recorded simultaneously with the electrochemical response over the same time intervals. The value of C_f was then calculated from the slope of the plot of the change in charge (Δq) versus the frequency change (Δf).

A mercury–mercurous sulfate electrode ($Hg/Hg_2SO_4/K_2SO_4$) and a spectroscopic-grade graphite rod (PARC) were used as the reference and counter electrodes, respectively. All potentials were measured with respect to mercury–mercurous sulfate electrode at room temperature. In the text, the potential values are referred to the normal hydrogen electrode (NHE). In order to minimize iR-drop effects, a Luggin capillary was employed to connect the reference-electrode compartment to the working-electrode one.

The solutions were prepared prior to each experiment using ultrapure water (18 MΩ cm), sulfuric acid (Backer), $ZnSO_4\cdot7H_2O$ (Backer), KCl (Backer). A stock BDA/EtOH solution containing 5 g of benzylideneacetone (BDA) ($C_6H_5CH=CHCOCH_3$) (Aldrich) and 100 ml of ethanol (EtOH) (Aldrich) was prepared (6 wt.% BDA in EtOH). All reagents were of analytic grade. Prior to each experiment, the solution in the cell was purged for 30 min

with ultrapure nitrogen (Praxair) and the experiments were carried out under a nitrogen atmosphere. In all experiments, the potential scans were performed over the potential range 0.06–1.5 V and were initiated in the negative direction beginning from the resting potential. The plots shown correspond to the first scan cycle.

3. Results and discussion

3.1. Electrochemical characteristics of the Pt-EQCM electrode in 0.5 M H_2SO_4

Before commencing the study of the UPD of Zn^{2+} ions and the influence of Cl^- and BDA/EtOH, the Pt-EQCM electrode was subjected to several potential cycles in the base solution S_0 of composition 0.5 M H_2SO_4. Fig. 1a shows a typical cyclic voltammogram (CV) of Pt in this medium [23,26,27]. Three characteristic potential regions are observed: region A (0.06–0.4 V), in which electroadsorption–electrodesorption of hydrogen (H UPD) occurs; region B (0.4–0.8 V) associated with the region of the double layer; region C (0.8–1.5 V) associated with the formation and reduction of platinum oxide (PtO) at the surface [27,28]. In region A, the process of H UPD is characterized by the cathodic peaks H_1^c and H_2^c associated with two types of adsorbed hydrogen (H_{ads}): strongly bound H and weakly bound H, respectively [29–32]. Peaks H_1^a and H_2^a are the anodic equivalents of H_1^c and H_2^c, respectively. Peak H_3^a corresponds to the desorption of H_{ads} from sites different from those described above. Recently, Jerkiewicz et al. [33,34] calculated the standard entropy of the UPD of H onto Pt (poly), $\Delta S_{Ads}^\circ(H_{ads})$, as a function of the surface coverage of H_{ads}, $\theta_{H_{ads}}$. The plot of $\Delta S_{Ads}^\circ(H_{ads})$ versus $\theta_{H_{ads}}$ revealed two waves, which the authors associated with two adsorption–desorption peaks in the CV profiles. In addition, they found that the $Pt–H_{ads}$ binding energy ($E_{Pt–H_{ads}}$) was in the range of 245–265 kJ mol^{-1}. The electric charge density
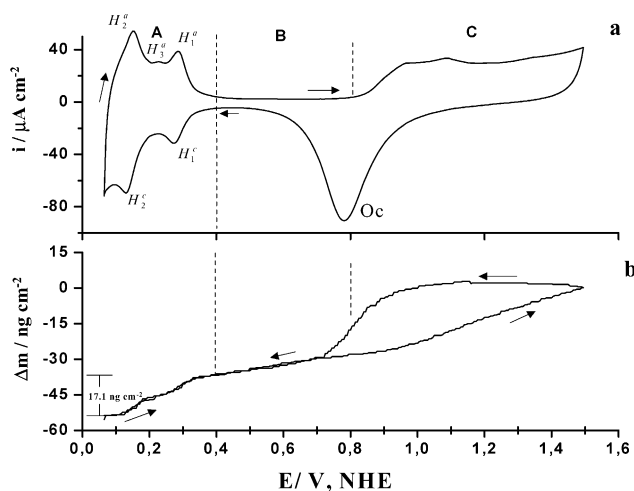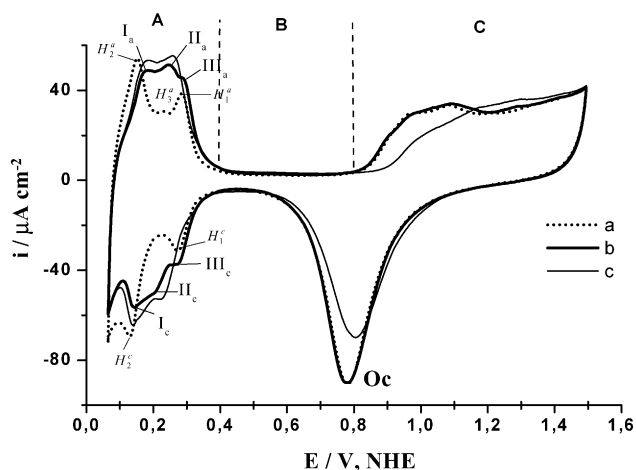
Fig. 2. Cyclic voltammograms of Pt-EQCM for three solutions: (a) S_0 (=0.5 M H_2SO_4), (b) S_1 (=$S_0 + 10^{-3}$ M Zn^{2+}) and (c) S_2 (=$S_1 + 10^{-4}$ M KCl). $v = 50$ mV s^{-1}.

for the desorption of hydrogen, obtained by integrating the i versus E curve in region A (anodic scan) was 0.175 mC cm^{-2} after correcting for the double layer charge.

Fig. 1b shows the variation in mass as a function of potential recorded simultaneously with the cyclic voltammogram in Fig. 1a. The offset $\Delta m = 0$ was fixed at $E = 1.5$ V. During the potential scan in the positive direction starting from 0.06 V, the mass (Δm) is observed to continuously increase in the potential range 0.06–1.5 V, with different values of the slope (dΔm/dE) in each potential region. In region A, the increase in mass (17.10 ± 0.57 ng cm^{-2}) has been attributed to the incorporation (adsorption) of water molecules during the desorption of H_{ads} (substitution of H_{ads} for the water molecule [35]); in region B, the increase in Δm has been associated with the incorporation of anions in the region of the double layer; and in region C, the increase in Δm has been attributed to the formation of PtO at the surface [27,28,36–38]. In a recent study using Auger electron spectroscopy, cyclic voltammetry and EQCN, Jerkiewicz et al. [27] generated a detailed description of the mass response of a cyclic voltammogram as part of the study of the formation of the surface oxide, PtO.

3.2. UPD of Zn on Pt in the absence and presence of Cl^- ions

Fig. 2 shows the CVs of Pt in the base solution S_0 (=0.5 M H_2SO_4) (curve a), in solution S_1 (=$S_0 + 10^{-3}$ M Zn^{2+}) (curve b), and in solution S_2 (=$S_1 + 10^{-4}$ M KCl) (curve c), recorded at 50 mV s^{-1}.

Comparison of the CVs obtained for solutions S_0 (curve a, Fig. 2) and S_1 (curve b, Fig. 2) shows the effect of the Zn^{2+} ions on H UPD. In the presence of Zn^{2+} ions (curve b), the anodic and cathodic current densities increase when $E < 0.3$ V (H UPD, zone A). The formation of three anodic peaks is observed (peak Ia, 0.2 V; peak IIa, 0.25 V; peak IIIa, 0.28 V) as well as the corresponding cathodic peaks (peak Ic, 0.16 V; peak IIc, 0.2 V; peak IIIc, 0.25 V). Peaks IIIc and

Fig. 1. (a) Cyclic voltammogram, and (b) Δm vs. E plot for a Pt-EQCM electrode in solution S_0 (=0.5 M H_2SO_4). $v = 50$ mV s^{-1}.
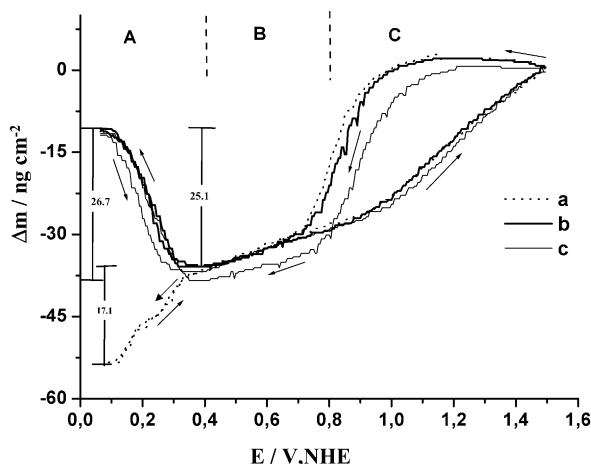
Fig. 3. Δm vs. E curves corresponding to the cyclic voltammograms in Fig. 2: (a) S_0 (=0.5 M H_2SO_4), (b) S_1 (=$S_0 + 10^{-3}$ M Zn^{2+}), (c) S_2 (=$S_1 + 10^{-4}$ M KCl). $v = 50$ mV s^{-1}.

IIIa are associated with the increase in the current density of peaks H_1^c and H_1^a, respectively, which correspond to the adsorption and desorption of strongly bound hydrogen [29–32] (Fig. 1). In addition, peaks Ic and Ia correspond to the decrease in the current density of peaks H_2^c and H_2^a, respectively, which are associated with the adsorption and desorption of weakly bound hydrogen [29–32] (Fig. 1). The anodic charge density ($Q_{F,A}^a$) in this potential range (0.06–0.4 V) was 0.205 ± 0.002 mC cm^{-2}. This value is 17% greater than that obtained in the absence of Zn^{2+} ions.

The data in Fig. 2 additionally indicate that the presence of Zn^{2+} ions has no significant effect on the processes in the region of the double layer electric charge (zone B) or on the formation and reduction of surface oxide (zone C). Similar results, showing an association between the changes observed in zone A of voltammograms with UPD of Zn^{2+} ions and the dissolution of Zn deposited by UPD, have been reported by Aramata et al. [15].

Introduction of Cl$^-$ ions into the solution (solution S_2) causes important changes in the voltammograms (curve c, Fig. 2). The voltammogram obtained in the presence of Cl$^-$ ions has the following features. In region A, only two cathodic peaks (Ic and IIc) and two anodic peaks (Ia and IIa) are observed. This behavior suggests that the Cl$^-$ ions inhibit both: the UPD of Zn^{2+} ions and H UPD associated with peak IIIc and promotes the process giving rise to peaks Ic and IIc in curve b. In addition, the current densities of these peaks are greater than those observed in the absence of Cl$^-$ ions (curve b). Moreover, the potential range corresponding to the charge of the double layer (zone B) increases; this effect is characteristic of the adsorption of Cl$^-$ [28] and is associated with the progressive blocking of the initial states (up to 0.85 V) of the formation of the PtO film [26–28,39]. This picture is corroborated by the decrease (23%) observed in the intensity of the peak corresponding to surface oxide reduction (peak O_c).

Fig. 3 shows the profiles of mass versus potential (Δm versus E) corresponding to the cyclic voltammograms in Fig. 2. Curves a–c in Fig. 3 have been grouped with an offset of $\Delta m = 0$ at the upper potential limit, $E = 1.5$ V. Curve a shows the change in mass as a function of potential for Pt in solution S_0. The behavior of this system was discussed above in relation to Fig. 1b; the data are included in Fig. 3 for comparison purposes. Comparison of the curves obtained for solutions S_0 and S_1 (curves a and b, respectively, Fig. 3) reveals that the mass changes in regions B and C do not depend on the presence of Zn^{2+} ions in the solution. However, in region A and in the presence of Zn^{2+} ions (curve b, Fig. 3), an increase (gain) in mass ($\Delta m_A^c = 25.10 \pm 0.57$ ng cm^{-2}) is observed during the potential scan in the negative direction. In addition, on switching the direction of the potential scan to the positive direction starting from 0.06 V, a decrease (loss) in mass of the same magnitude is observed ($\Delta m_A^a = -25.10 \pm 0.57$ ng cm^{-2}), suggesting that in this potential range the process of Zn deposition and dissolution is reversible.

The voltammetry results indicate that the dissolution of Zn deposited by UPD occurs simultaneously with hydrogen desorption. Thus, the experimentally determined mass change during the potential scan in the positive direction ($\Delta m_A^a = 25.10 \pm 0.57 =$ ng cm^{-2}) will depend on two factors: mass loss due to the dissolution of Zn deposited by UPD ($\Delta m_{diss,upd}^{Zn}$) and mass gain due to the adsorption of water molecules ($\Delta m_{ads}^{H_2O} = 17.10 \pm 0.57$ ng cm^{-2}) during the process of hydrogen desorption from the Pt surface (Fig. 1b).

Considering that the masses of H_2O and $H_2O + H_{ads}$ cannot be distinguished within the error of this experiment, the total mass of dissolution of Zn deposited by UPD was determined using the following equation:

$$\Delta m_A^a = \Delta m_{diss,upd}^{Zn} + \Delta m_{ads}^{H_2O} \tag{2}$$

where Δm_A^a is the net decrease in mass recorded by EQCM ($= -25.10 \pm 0.57$ ng cm^{-2}) during the positive scan in region A, $\Delta m_{ads}^{H_2O}$ is the mass of adsorbed water molecules (17.10 ± 0.57 ng cm^{-2}), and $\Delta m_{diss,upd}^{Zn}$ is the total mass of dissolution of Zn deposited by UPD. The absolute value of $\Delta m_{diss,upd}^{Zn}$ obtained was 42.20 ± 0.57 ng cm^{-2}. The electric charge density associated with the total dissolved mass ($\Delta m_{diss,upd}^{Zn}$), $Q_{diss,upd}^{Zn} = 0.124 \pm 0.002$ mC cm^{-2}, is less than that obtained by voltammetry for the same process ($Q_{F,A}^a = 0.205 \pm 0.002$ mC cm^{-2}). The excess electric charge is associated with the charge due to hydrogen desorption from the Pt surface ($Q_{upd}^H = Q_{F,A}^a - Q_{diss,upd}^{Zn} = 0.081$ mC cm^{-2}).

From the EQCM results, and assuming complete discharge of the Zn^{2+} ions [15,16,19] the surface coverage of the zinc, θ_{Zn-upd}, can be evaluated using the following equation, which is valid in the potential range of 0.06–0.4 V:

$$\theta_{Zn-upd} = \left(\frac{Q_{diss,upd}^{Zn}}{2Q_{H,s}} \right) = 0.29 \tag{3}$$

where $Q_{\text{diss,upd}}^{\text{Zn}}$ is the anodic charge density associated with the dissolution of Zn adatoms, $Q_{\text{H,s}}$ the charge density associated with the adsorption of a H monolayer onto polycrystalline Pt (0.210 mC cm^{-2}) and a transfer of two electrons from the Zn [15,16,19].

Curve c in Fig. 3 shows the effect of adding Cl$^-$ ions (solution S$_2$) on the UPD of Zn^{2+} ions. The mass changes produced in potential regions B and C of the Δm versus E curve (curve c, Fig. 3) are similar to those reported by Zolfaghari at al. [28] for Pt in 0.05 M H$_2$SO$_4$ in the presence of Cl$^-$ ions. Specifically, when Cl$^-$ ions are present in the solution a hysteresis is observed in the double layer region (region B) between the potential scans in the positive and negative directions. This behavior is attributed to transitory desorption of Cl$^-$ due to reduction of coadsorbed O species generated during the anodic scan. At more positive potentials (region C), the adsorbed Cl$^-$ ions inhibit the surface oxide formation during the positive potential scan; as a result, the mass changes due to the formation and reduction of surface oxide are smaller in the presence of Cl$^-$ ions than in their absence.

In region A, during the potential scan in the negative direction, the Δm versus E curve shows a mass increase of 26.70 ± 0.57 ng cm^{-2} in the potential range of 0.40–0.06 V. This implies that the presence of Cl$^-$ ions causes a mass increase 6% greater than that observed in the absence of Cl$^-$ ions. However, on switching the potential scan to the positive direction starting from 0.06 V, a mass loss of 25.10 ± 0.57 ng cm^{-2} is observed in the same potential range. This value is similar to that obtained in the absence of Cl$^-$ ions (curve b, Fig. 3), which suggests that the quantity of Zn deposited does not depend on the presence of Cl$^-$ ions in the solution. The mass of adsorbed species that are not desorbed during the potential scan in the positive direction (1.6 ng cm^{-2}) may be associated with the adsorption of Cl$^-$ ions onto the electrode surface that then remain on the electrode surface [19,20,28], causing a hysteresis between the deposition and dissolution of Zn (curve c, Fig. 3). Thus, the increase in charge observed in the voltammogram recorded in the presence of ions chloride (curve c, Fig. 2) corresponds to an increase in the quantity of H$_{\text{ads}}$ and not to UPD of Zn^{2+} ions.

3.3. Effect of BDA/EtOH and Cl$^-$ ions on the UPD of Zn on Pt

The influence of BDA/EtOH on the UPD of Zn^{2+} ions onto Pt was analyzed using solutions comprised of solution S$_2$ with different concentrations of BDA/EtOH ($6.8 \times 10^{-7} \leq$ [BDA] $\leq 2.7 \times 10^{-6}$ M and its corresponding concentrations of EtOH ($3.4 \times 10^{-5} \leq$ [EtOH] $\leq 1.3 \times 10^{-4}$ M)). The potential scans were performed in the negative direction starting from the resting potential. Prior to each experiment, the Pt-EQCM electrode was regenerated in solution S$_0$ to ensure that it was clean.
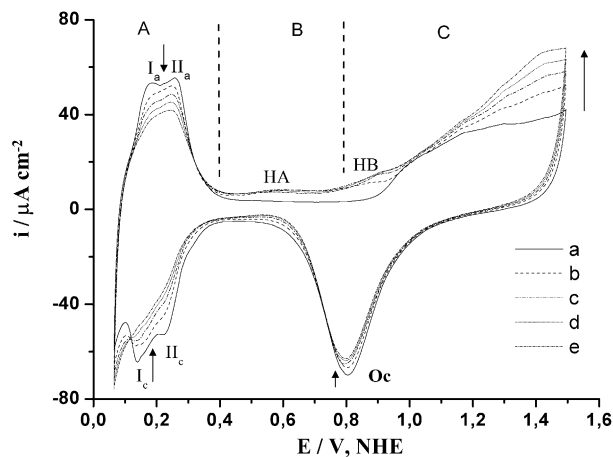
Fig. 4. Cyclic voltammograms of Pt-EQCM in solution S$_2$ (=0.5 M H$_2$SO$_4$ + 10^{-3} M Zn^{2+} + 10^{-4} M KCl) with different concentrations of BDA/EtOH: (a) 0.0, (b) 6.8×10^{-7} M BDA/3.4×10^{-5} M EtOH, (c) 1.36×10^{-6} M BDA/6.86×10^{-5} M EtOH, (d) 2.05×10^{-6} M BDA/1×10^{-4} M EtOH, (e) 2.7×10^{-6} M BDA/1.37×10^{-4} M EtOH. $v = 50$ mV s^{-1}.

Fig. 4 shows the cyclic voltammograms of Pt in solution S$_2$ containing different concentrations of BDA/EtOH. The presence of BDA/EtOH in the solution significantly modifies the voltammograms. In region A, as the concentration of BDA/EtOH in the solution is increased, a progressive decrease is observed in the intensities of the cathodic and anodic peaks (I and II) corresponding to the UPD of Zn^{2+} ions and the dissolution of Zn deposited by UPD, respectively, indicating that BDA/EtOH partially inhibits the UPD of Zn^{2+} ions. Additionally, the cathodic current at the lower potential limit (0.06 V) increases with increasing BDA/EtOH concentration.

The inhibition of the UPD of Zn^{2+} ions by the adsorption of BDA/EtOH can be utilized to estimate the degree of blocking of the Pt surface by the additive, using the following equation:

$$\Theta_{\text{blo}} = \frac{Q_{\text{F,A}}^{\text{a}} - Q_{\text{F,A}}^{\text{a,BDA}}}{Q_{\text{F,A}}^{\text{a}}} \tag{4}$$

where $Q_{\text{F,A}}^{\text{a}}$ and $Q_{\text{F,A}}^{\text{a,BDA}}$ are the anodic electric charge densities in region A in the absence and presence of BDA/EtOH, respectively. Both charges were measured from the voltammograms shown in Fig. 4. The difference between $Q_{\text{F,A}}^{\text{a}}$ and $Q_{\text{F,A}}^{\text{a,BDA}}$ is proportional to the number of sites blocked by BDA/EtOH. The value of Θ_{blo} increases with increasing BDA/EtOH concentration, up to 0.37 at the highest BDA/EtOH concentration studied (see Table 1). This behavior can be explained by considering that, as for most additives, BDA is adsorbed on the cathode. Using IR and ^{1}H NMR spectroscopy, Mockute et al. [10,12] showed that during the electrolysis of Zn in baths containing BDA/EtOH, the additive decomposes into diverse compounds, including benzylacetone (BAC), benzaldehyde (BZ), and 1-phenylbutanol-3 (FL). They proposed that BAC is formed at the cathode by reduction of BDA, and that BAC is subsequently reduced to FL, with this process likely being accelerated by the pro-

Table 1
Influence of the concentration of BDA/EtOH on the anodic charge of Pt in solution S_2 (=0.5 M H_2SO_4 + 10^{-3} M Zn^{2+} + 10^{-4} M KCl) in different regions of the voltammogram

[BDA]/[EtOH] ($\times 10^5$ mol l^{-1})	$Q_{F,A}^{a,BDA}$ (± 0.002 mC cm^{-2})	Θ_{blo}	$Q_{F,(0.4-1.5\,V)}^{a,BDA}$ (± 0.002 mC cm^{-2})	% $Q_{F,(0.4-1.5\,V)}^{a,exc}$
0.068/3.43	0.164	0.20	0.445	26.19
0.137/6.86	0.146	0.28	0.510	44.54
0.200/10.0	0.135	0.34	0.521	47.46
0.270/13.7	0.129	0.37	0.547	54.88

$Q_{F,A}^a = 0.205 \pm 0.002$ mC cm^{-2}, $Q_{F,(0.4-1.5\,V)}^a = 0.354 \pm 0.002$ mC cm^{-2}.

tonation of the carbonyl group of BAC. On the other hand, BZ is formed in the cathodic layer, where the pH is higher than in the solution. In addition, the reduction of EtOH occurs at $E < 0.3$ V; Schmidt et al. [40] proposed that this process proceeds via a strong interaction of ethanol with the electrode/electrolyte interface, leading to the formation of adsorbed intermediates that react with adsorbed hydrogen atoms. Thus, the additive BDA/EtOH or the reaction products partially block the activated sites on the Pt surface for the adsorption of H and the UPD of Zn^{2+} ions.

During the potential scan in the positive direction, in region B (0.4–1.0 V) the presence of BDA/EtOH causes an increase in the current density with respect to that observed in the absence of BDA/EtOH (curve a, Fig. 4). Two current density bands are observed, one between 0.4 and 0.7 V (HA), whose intensity is independent of the concentration of BDA/EtOH, and another between 0.85 and 1.0 V (HB), whose intensity increases slightly with increasing BDA/EtOH concentration. At more positive potentials (region C, 1.0–1.5 V), a progressive increase is observed in the current density as the concentration of BDA/EtOH is increased. In the potential range 0.4–1.5 V, the anodic charge density obtained in the presence of BDA/EtOH ($Q_{F,(0.4-1.5\,V)}^{a,BDA}$) was between 26 and 54% greater (% $Q_{F,(0.4-1.5\,V)}^{a,exc}$) than that obtained in the absence of the additive ($Q_{F,(0.4-1.5\,V)}^a$) (Table 1).

On switching the potential scan to the negative direction starting from 1.5 V, a cathodic peak, O_c, is observed at 0.8 V, associated with the reduction of the surface oxide (Fig. 4). The intensity of this cathodic peak decreases only slightly (<10%) when BDA/EtOH is added to the solution. This suggests that the oxidation products formed in regions B and C during the positive potential scan are produced simultaneously in the presence of adsorbed Cl$^-$ ions and with the formation of surface oxide. Thus, the present findings suggest that there is no interference between the BDA/EtOH and the Cl$^-$ ions.

The behavior observed in regions B and C of the voltammograms in Fig. 4 is characteristic of the oxidation reactions of ethanol on platinum electrodes in acidic media [40–45]. Previous studies by Schmidt et al. [40] indicate that the oxidation of EtOH (0.01 M) on Pt/HClO$_4$ (1 M) commences at 0.42 V during the positive potential scan. Analyses of the products of the oxidation of ethanol on Pt by Fourier transform infrared spectroscopy (FT-IRS) [40–42] and on-line differential electrochemical mass spectroscopy (DEMS) [43,44]

have identified ethanal, acetic acid and CO$_2$ as products of this reaction.

Fig. 5 shows a series of Δm versus E plots obtained simultaneously with the voltammograms in Fig. 4 at various concentrations of BDA/EtOH. For comparison purposes the offset $\Delta m = 0$ was fixed at the upper potential limit (1.5 V). In region A, Δm increases (mass gain) during the potential scan in the negative direction and decreases (mass loss) ($\Delta m_A^{a,BDA}$) during the scan in the positive direction, indicating that the process UPD of Zn^{2+} ions occurs in the presence of Cl$^-$ ions and BDA/EtOH.

From the plot of Δm versus E recorded in the absence of BDA (Fig. 1b), the quantity of water adsorbed in the potential range of 0.06–0.4 V can be estimated as 17.1 ng cm^{-2}. In addition, considering that only a fraction of hydrogen adsorption sites (H sites) are blocked by the presence of BDA/EtOH in the solution, and that the remaining sites can adsorb water molecules ($\Theta_{ads}^{H_2O} = 1 - \Theta_{blo}$), it is possible to determine the quantity of adsorbed water as a function of the adsorbed fraction of BDA/EtOH: $\Delta m_{ads}^{H_2O,BDA} = 17.1 \times (1 - \Theta_{blo})$. The values of $\Delta m_{ads}^{H_2O,BDA}$ obtained at different BDA/EtOH concentrations are listed in Table 2. Besides, Table 2 shows the mass change due to dissolution of Zn deposited by UPD
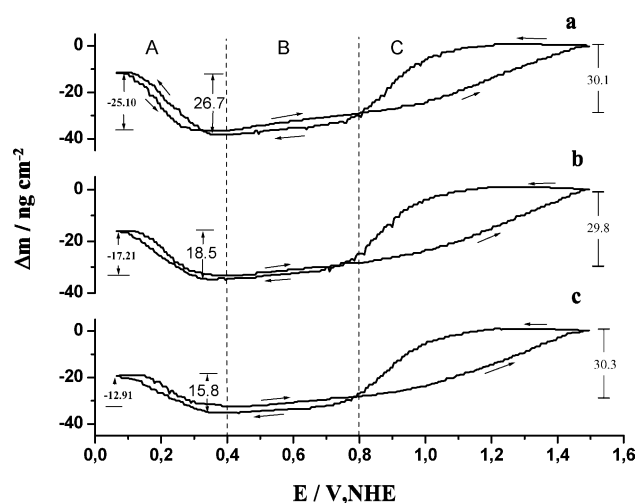
Fig. 5. Δm vs. E curves for Pt in solution S_2 (=0.5 M H_2SO_4 + 10^{-3} M Zn^{2+} + 10^{-4} M KCl) with different concentrations of BDA/EtOH corresponding to the cyclic voltammograms in Fig. 4: (a) absence of BDA/EtOH, (b) 1.36×10^{-6} M BDA/6.86×10^{-5} M EtOH, and (c). 2.7×10^{-6} M/1.37×10^{-4} M EtOH. $v = 50$ mV s^{-1}.

Table 2
Influence of the concentration of BDA/EtOH on the mass of Zn deposited by UPD and surface coverage

[BDA]/[EtOH] ($\times 10^5$ mol l^{-1})	$\Delta m_A^{a,BDA}$ (± 0.57 ng cm^{-2})	$\Delta m_{Ads}^{H_2O,BDA}$ (± 0.57 ng cm^{-2})	$\Delta m_{diss,upd}^{Zn,BDA}$ (± 0.57 ng cm^{-2})	$\Delta m_{dep,upd}^{Zn,BDA}$ (± 0.002 mC cm^{-2})	$Q_{diss,upd}^{Zn,BDA}$ (± 0.57 mC cm^{-2})	θ_{Zn-upd}^{BDA}
0.068/3.43	−20.27	13.68	−33.95	35.02	0.100	0.23
0.137/6.86	−17.21	12.14	−29.35	30.63	0.086	0.20
0.200/10.0	−14.44	11.29	−25.73	28.05	0.075	0.17
0.270/13.70	−12.91	10.80	−23.71	26.63	0.069	0.16

$\Delta m_{dep,upd}^{Zn} = 43.8 \pm 0.57$ ng cm^{-2}, $\Delta m_{diss,upd}^{Zn} = -42.2 \pm 0.57$ ng cm^{-2}.

($\Delta m_{diss,upd}^{Zn,BDA}$), evaluated from $\Delta m_A^{a,BDA}$ using the following equation:

$$\Delta m_A^{a,BDA} = \Delta m_{diss,upd}^{Zn,BDA} + \Delta m_{ads}^{H_2O,BDA} \qquad (5)$$

where $\Delta m_A^{a,BDA}$ is the net decrease in mass recorded by EQCM during the positive scan in region A at a particular BDA/EtOH concentration (Table 2), $\Delta m_{ads}^{H_2O,BDA}$ is the mass of adsorbed water molecules, and $\Delta m_{diss,upd}^{Zn,BDA}$ is the total mass of dissolution of Zn deposited by UPD.

Increasing the concentration of BDA/EtOH causes a decrease in the absolute value of $\Delta m_{diss,upd}^{Zn,BDA}$, that is, in the quantity of Zn deposited by UPD. At the highest BDA/EtOH concentration studied (2.7×10^{-6} MBDA/1.37×10^{-4} MEtOH), the absolute value of $\Delta m_{diss,upd}^{Zn,BDA}$ was 23.71 ± 0.57 ng cm^{-2}, which is 44% less than the mass change observed in the absence of BA/EtOH (42.20 ± 0.57 ng cm^{-2}). In addition, it is important to observe that at a particular BDA/EtOH concentration, the absolute value of $\Delta m_{diss,upd}^{Zn,BDA}$ is less than that due to the UPD of Zn^{2+} ions ($\Delta m_{dep,upd}^{Zn,BDA}$), and that this difference increases with increasing BDA/EtOH concentration. This suggests that the UPD of Zn^{2+} ions occurs at the same time as the adsorption of one or more other species from the medium or reaction products that remain on the electrode surface during the dissolution of Zn deposited by UPD (e.g. Cl$^-$ ions or products of reactions of the BDA/EtOH mixture). In addition, the values of the charge density ($Q_{diss,upd}^{Zn,BDA}$) (Table 2) obtained using the total dissolved mass at the various BDA concentrations ($\Delta m_{diss,upd}^{Zn,BDA}$) are less than the corresponding values obtained by voltammetry (Fig. 4) ($Q_{F,A}^{a,BDA}$; Table 1). This excess charge is associated with the charge due to the desorption of hydrogen (H$_{ads}$) from the Pt surface.

In region C (0.8–1.5 V), the mass change due to the formation and reduction of surface oxides is approximately the same ($\cong 30.00 \pm 0.57$ ng cm^{-2}) in the absence (curve a, Fig. 5) and presence (curves b and c. Fig. 5) of BDA/EtOH, indicating that the quantity of surface oxide (PtO) formed does not depend on the concentration of BDA/EtOH in solution. This result is similar to that observed by voltammetry (peak O$_c$, Fig. 4).

Comparison between the voltammograms (Fig. 4) and the Δm versus E plots (Fig. 5) shows that there is no mass change

corresponding to the charge density observed in regions B and C. This suggests that in these potential regions a Faradaic process takes place during the positive potential scan that does not involve a mass change. In agreement with Iwasita et al. [46], oxidative ethanol adsorption on Pt electrodes takes place in two separate potential regions: 64% of the adsorbates are oxidized below a maximum at 0.70–0.80 V, and the oxidation of the remaining intermediates leads to a broad current peak superimposed on the peak associated with platinum oxide formation. CO$_2$ and ethanal have been identified as oxidation products [40]. In agreement with Snook et al. [47], the processes that involve gas-phase species make an insignificant contribution to the mass-potential response. However, these processes make a significant contribution in the voltammogram.

Table 2 shows the surface coverage of zinc adatoms (θ_{Zn-upd}^{BDA}) as a function of the concentration of BDA/EtOH, evaluated based on the anodic charge density associated with the mass of the Zn deposited by UPD that was dissolved during the positive scan ($Q_{diss,upd}^{Zn,BDA}$) using Eq. (3). The surface coverage of zinc decreases with increasing concentration of BDA/EtOH in the solution.

The inhibition of the UPD of Zn^{2+} ions by BDA/EtOH is an interesting result from a technological viewpoint because in general the UPD of metals plays a fundamental role in the anomalous codeposition of alloys [48]. Thus, the inhibition of the UPD of Zn^{2+} ions could potentially be exploited to modify the mechanism of the anomalous codeposition of Zn alloys (e.g., Zn–Co [14]).

4. Conclusions

The influence of Cl$^-$ ions and BDA/EtOH on UPD of Zn^{2+} ions was investigated by EQCM and voltammetry. The results show that the process UPD of Zn^{2+} ions occurs simultaneously with H UPD. The maximum surface coverage of the Zn onto Pt (0.29) was obtained in the absence of Cl$^-$ and BDA/EtOH. In addition, the EQCM study revealed that the presence of Cl$^-$ ions does not interfere with the UPD of Zn^{2+} ions. However, Cl$^-$ ions remain adsorbed on the Pt surface, inhibiting the formation of surface oxides (PtO).

In the presence of BDA/EtOH, oxidation of EtOH was observed during the positive potential scan in regions corresponding to the electric charge of the double layer and to the

formation of PtO. The experiments additionally revealed that the additive BDA/EtOH does not interfere with the adsorption of Cl$^-$ or the formation of surface oxides.

The EQCM study in the UPD region of the voltammograms showed that the presence of BDA/EtOH reduced the quantity of Zn deposited by UPD by up to 44%, an effect that is associated with the adsorption of BDA/EtOH or reaction products onto the Pt surface.

The inhibition of the UPD of Zn^{2+} ions by BDA/EtOH may have important technological implications because the UPD of metals plays an important role in the anomalous codeposition of alloys. Thus, addition of BDA/EtOH to inhibit the UPD of Zn^{2+} ions could partially inhibit the anomalous codeposition of Zn alloys (e.g., Zn–Fe, Zn–Ni and Zn–Co), making it possible to obtain Zn alloy coatings of more homogeneous composition.

Acknowledgement

References

[1] G. Barceló, M. Sarret, C. Müller, J. Pregonas, Electrochim. Acta 43 (1988) 13.
[2] S. Rajendran, S. Bharanti, C. Krishna, Plat. Surf. Finish. 84 (1997) 53.
[3] A.Y. Hosny, M.E. El-Rofei, T.A. Ramadan, B.A. El-Gafari, Met. Finish. 93 (1995) 55.
[4] B. Bozzini, V. Accardi, P.L. Cavalloti, F. Pavan, Met. Finish. 97 (1999) 33.
[5] G. Trejo, R. Ortega Borges, Y.V. Meas, E. Chainet, B. Nguyen, P. Ozil, J. Electrochem. Soc. 145 (1998) 4090.
[6] D.D.N. Singh, M. Dey, V. Singh, Corrosion 58 (2002) 971.
[7] M. Sanchez Cruz, F. Alonso, J.M. Palacios, J. Appl. Electrochem. 23 (1993) 364.
[8] J. Yu, H. Yang, X. Ai, Y. Chen, Russ. J. Electrochem. 38 (2002) 363.
[9] D.S. Baik, D.J. Fray, J. Appl. Electrochem. 31 (2001) 1141.
[10] D. Mockute, G. Bernotiene, Chemija 2 (1996) 90.
[11] G. Bernotiene, D. Mockute, Chemija 2 (1994) 3.
[12] D. Mockute, G. Bernotiene, J. Appl. Electrochem. 27 (1997) 691.
[13] V. Danciu, V. Cosoveanu, E. Grunwald, G. Oprea, Galvanotechnik 94 (2003) 566.
[14] G. Trejo, R. Ortega, Y. Meas, E. Chainet, P. Ozil, J. Appl. Electrochem. 33 (2003) 373.
[15] D.A. Quaaiyyum, A. Aramata, S. Moniwa, S. Sathochi, M. Enyo, J. Electroanal. Chem. 373 (1994) 61.
[16] A. Aramata, Md.A. Quaiyyum, W.A. Balais, T. Atoguchi, M. Enyo, J. Electroanal. Chem. 338 (1992) 367.
[17] S. Taguchi, A. Aramata, Md.A. Quaaiyyum, M. Enyo, J. Electroanal. Chem. 374 (1994) 275.
[18] S. Taguchi, A. Aramata, J. Electroanal. Chem. 396 (1995) 131.
[19] G. Horanyi, A. Aramata, J. Electroanal. Chem. 434 (1997) 201.
[20] G. Horanyi, A. Aramata, J. Electroanal. Chem. 437 (1997) 259.
[21] A. Aramata, S. Teuri, S. Taguchi, T. Kawaguchi, K. Shimazu, Electrochim. Acta 41 (1996) 761.
[22] L.H. Mascaro, M.C. Santos, S.A.S. Machado, L.A. Avaca, J. Braz. Chem. Soc. 13 (2002) 529.
[23] R. Woods, in: A.J. Bard (Ed.), Electroanalytical Chemistry, vol. 9, Marcel Dekker, New York, 1977, p. 1.
[24] G. Sauerbrey, Z. Phys. 155 (1959) 206.
[25] G. Vatankhah, J. Lessard, G. Jerkiewicz, A. Zolfaghari, B.E. Conway, Electrochim. Acta 48 (2003) 1613.
[26] I. Bakos, G. Horanyi, J. Electroanal. Chem. 332 (1992) 147.
[27] G. Jerkiewicz, G. Vatankhah, J. Lessard, M. Soriaga, Yeon-Su, Electrochim. Acta 49 (2004) 1451.
[28] A. Zolfaghari, B.E. Conway, G. Jerkiewicz, Electrochim. Acta 47 (2002) 1173.
[29] A. Bewick, A.M. Taxford, J. Electroanal. Chem. 47 (1973) 255.
[30] A. Bewick, J.W. Russell, J. Electroanal. Chem. 132 (1982) 329.
[31] A. Bewick, J.W. Russell, J. Electroanal. Chem. 132 (1982) 337.
[32] R.J. Nichols, A. Bewick, J. Electroanal. Chem. 243 (1988) 445.
[33] A. Zolfaghari, M. Chayer, G. Jerkiewicz, J. Electrochem. Soc. 144 (1997) 3034.
[34] A. Zolfaghari, G. Jerkiewicz, J. Electroanal. Chem. 467 (1999) 177.
[35] F. Gloaguen, J.-M. Léger, C. Lamy, J. Electroanal. Chem. 467 (1999) 186.
[36] M.C. Santos, L.O.S. Bulhoes, Electrochim. Acta 18 (2003) 2607.
[37] K. Shimazu, H. Kita, J. Electroanal. Chem. 341 (1992) 361.
[38] M.C. Santos, D.W. Miwa, S.A.S. Machado, Electrochem. Commun. 2 (2000) 692.
[39] D.M. Novak, B.E. Conway, J. Chem Soc., Faraday Trans. 77 (1981) 2341.
[40] V.M. Schmidt, R. Ianniello, E. Pastor, S. González, J. Phys. Chem. 100 (1996) 17901.
[41] C. Yañez, C. Gutiérrez, M.S. Ureta-Zañartu, J. Electroanal. Chem. 541 (2003) 39.
[42] L.-W. Leung, S.-C. Chang, M.J. Weaver, J. Electroanal. Chem. 266 (1989) 317.
[43] A.T. Iwasita, B. Rasch, E. Cattaneo, W. Vielstich, Electrochim. Acta 34 (1989) 1073.
[44] J. Willsau, J. Heitbaum, J. Electroanal. Chem. 194 (1985) 27.
[45] B. Bittins-Cattaneo, S. Wilhem, E. Cattaneo, H.W. Buschmann, W. Vielstich, Phys. Chem. 92 (1988) 1210.
[46] T. Iwasita, E. Pastor, Electrochim. Acta 39 (1994) 531.
[47] G.A. Snook, A.M. Bond, S. Fletcher, J. Electroanal. Chem. 526 (2002) 1.
[48] M.J. Nicol, H.I. Philip, J. Electroanal. Chem. 70 (1976) 233.